Macromolecular Research (2024) 32:861–872
https://doi.org/10.1007/s13233-024-00266-6

Online ISSN 2092-7673
Print ISSN 1598-5032

ARTICLE

Chitosan-reinforced nanocrystalline cellulose hydrogels containing activated carbon as antitoxin wound dressing

Najihah Rameli[1] · Bee-Yee Lim[1] · Pei-Yee Leong[1] · Choon-Choo Lim[2] · Shiow-Fern Ng[1]

Received: 4 January 2024 / Revised: 20 March 2024 / Accepted: 7 April 2024 / Published online: 10 May 2024

Abstract

Wound infection causes wound chronicity as the presence of pathogens prolong wound healing time. Endotoxins lipopolysaccharides (LPS) are released from Gram-negative bacteria when they are lysed by host phagocytic cells during an immune response. These endotoxins in wounds are shown to be one of the causes of delayed wound healing. The porous activated carbon (AC) can act as an important absorptive material for the elimination of bacterial toxins, which makes it an attractive biomaterial for infected wounds. NCC is also reported to facilitate cell adhesion, proliferation, and migrations. Previously, our laboratory has shown that chitosan (CS) reinforced with Kenaf nanocrystalline celluloses (NCC) possesses vastly improved mechanical properties. This study explores the potential of incorporating AC into NCC-CS hydrogel (AC/NCC), with the aim of eliminating bacteria toxins in wounds as well as the acceleration of wound healing. The AC/NCC hydrogel was characterized in terms of rheological properties, swelling behaviour, fourier transform infrared spectroscopy as well as zeta potential. Then the AC/NCC hydrogel dressings were evaluated in vitro using a cytotoxicity study and toxin removal assay. The results showed that hydrogels exhibit desirable rheological properties with homogenous activated carbon particles. The hydrogels exhibit low cytotoxicity towards the human fibroblast and keratinocytes cells. The hydrogel can remove up to 85% of endotoxins when treated with 0.1 EU/mL of LPS. In summary, this study has shown that AC/NCC hydrogel has a vast potential as an antitoxin dressing for infected chronic wounds.

✉ Shiow-Fern Ng
nsfern@ukm.edu.my; nsfern@gmail.com

[1] Faculty of Pharmacy, Centre for Drug Delivery Technology and Vaccine, Universiti Kebangsaan Malaysia, 50300 Kuala Lumpur, Malaysia

[2] Noble Healthcare, H-0-6, M Avenue, No.1, Jalan 1/38A, Segambut Bahagia, 51200 Kuala Lumpur, Malaysia

Graphical Abstract

AC/NCC hydrogel dressing eliminates endotoxin from infected wounds and accelerates wound healing

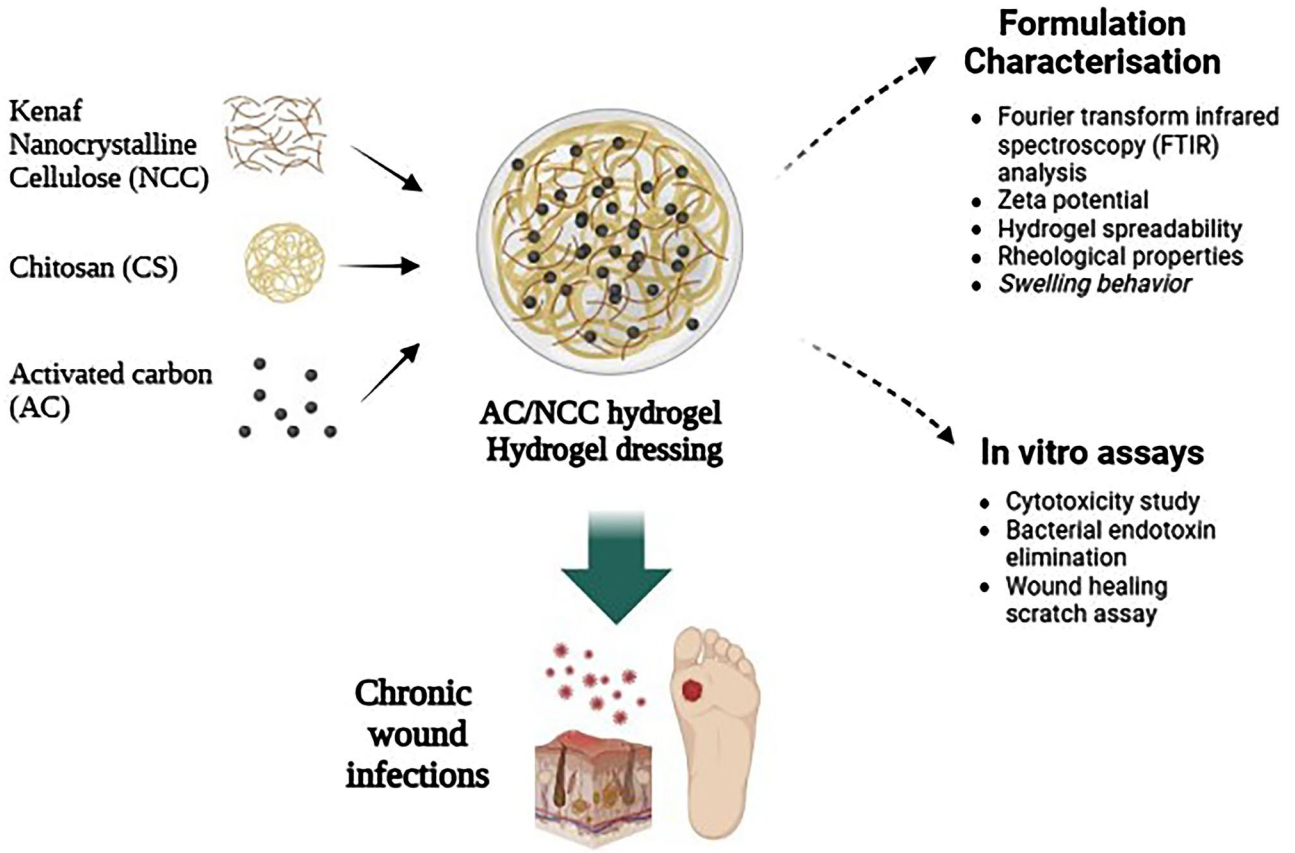

Keywords Activated carbon · Nanocrystalline cellulose · Bacterial toxins · Wound healing · Antitoxin wound dressing

1 Introduction

Chronic wounds are one of the problem due to their increasing morbidity rate which creates a financial impact to healthcare economy [1]. Wound infection remains the main cause of wound chronicity since chronic wounds are typically more easily infected by bacteria and pathogens as it prolongs healing time. Wound infection occurs when the bacteria continue to proliferate and invade the deeper wound, which consists of healthy viable tissue. In a chronic and infected wound, bacterial toxins are known as one of the causes of the delayed wound healing process [2]. Endotoxins lipopolysaccharides (LPS) are released from Gram-negative bacteria when they are lysed by host phagocytic cells during an immune response, or by antimicrobial agents. LPS induce the release of a large number of inflammatory mediators, inducing continuous inflammation at the infected site [3] and thus inhibiting wound healing, leading to chronic wounds and, in extreme cases, life-threatening sepsis. These endotoxins have the potential to interfere with the healing process, causing chronic wounds to take longer to heal.

For years, charcoal has been used as an antidote for food poisoning. Activated carbon (AC), like charcoal is produced carbon-rich materials such as coconut shells, rice husk and wood pulps that has been heated and turned into a powder. The process makes AC a highly porous material, with a large surface area, as well as high adsorption ability. AC has been widely used in a variety of industries [4–6] particularly in wastewater treatment [7–9]. Wound dressings that contain AC provide odour management to tackle foul-smelling wounds and help to prevent sepsis in some cases [10]. In wound care management, porous AC can act as an important absorptive material for the elimination of bacterial toxins, which makes it an ideal biomaterial for the treatment of infected wounds. A randomized controlled clinical trial [11] was conducted to investigate the potential usefulness of using AC impregnated with silver in the management of chronic wounds. Compared with the baseline, the

mean percentage reduction in wound area was statistically significant for the treatment group (28.7% ± 3.9%) versus the control (11.7% ± 6.8%). The test dressing was also found to reduce exudate levels, malodor and oedema. The clinical data indicated that the AC with silver dressing may help remove toxins from the wound bed fluid that impair the healing process [11]. In another study, mesoporous AC has been reported to remove endotoxins and inflammatory cytokine from fluid in vitro [12]. When submerged in a milieu enriched with *E. coli*, AC is effective at removing 90–95% of this toxin [13]. In experiments using a murine model of gut-derived endotoxemia, AC was able to bind endotoxin in the test methods [14]. Additionally, it also has been shown that AC can adsorb bacteria, viruses and various other biochemicals [12, 15].

Recently, nanocrystalline celluloses (NCC) have gained much attention experimentally in the field of tissue engineering, drug delivery and functional materials for wound dressing [16–22]. Heimbuck et al. [23] have found that chitosan (CS) hydrogel cross-linked with genipin is able to absorb large quantities of fluid (~ 230%) which is a potential dressing for highly exudating wounds such as infected chronic wounds. The intrinsic antimicrobial activity of CS is also shown to exhibit bactericidal actions in wounds [24]. In our laboratory, we successfully synthesised NCC from kenaf biowaste and our study also showed that the CS hydrogel reinforced with NCC possesses vastly improved mechanical properties [17]. Besides, owing to its nanosized properties, NCC in the hydrogel is reported to influence cell adhesion, proliferation, migration and cell differentiations [25, 26]. These features are vital for cell proliferation and tissue growth in wound healing and hence NCC-CS hydrogel has become a very appealing biomaterial composite for wound dressing formulation [19].

This current study explores the use of AC loaded onto NCC-CS as a hydrogel carrier. The kenaf NCC synthesis will be based on a method produced in our laboratory [17]. This hydrogel composite is formulated with the aim of eliminating bacteria toxins in wounds as well as the acceleration of wound healing. The objective of this study was firstly to formulate a CS-NCC hydrogel for wound dressing incorporated AC. Then, the physico-mechanical properties of the hydrogels were investigated and finally the cytotoxicity to human dermal fibroblast and the bacterial toxin removal ability of the hydrogels were examined in vitro.

2 Experimental

2.1 Materials

Kenaf bast fibers were obtained from the National Kenaf and Tobacco Board (LKTN). AC was a gift from Noble Health Sdn Bhd, Malaysia. Sodium hydroxide (NaOH), sodium chlorite ($NaClO_2$), sulphuric acid (H_2SO_4), low molecular weight CS (M_w 50–190 kDa with a degree of deacetylation of 75–85%) and genipin was procured from Sigma-Aldrich (UK). Glacial acetic acid used for the bleaching process was purchased from Merck (USA). Gelatine was purchased from Fluka Analytical (Darmstadt, Germany). Intrasite Gel Hydrogel Dressing (Smith & Nephew) was purchased from a local pharmacy in Malaysia.

Escherichia coli (*E. coli*) ATCC 25927 was obtained from the microbiology laboratory, Faculty of Pharmacy, Universiti Kebangsaan Malaysia (UKM). For toxicity testing, normal human dermal fibroblasts (NHDF) and normal human epidermal keratinocytes were purchased from Lonza (US). Dulbecco's modified Eagle's medium (DMEM), antibiotics (streptomycin and penicillin) and dimethyl sulfoxide (DMSO), 25% of acetic acid were obtained from Sigma Alrich (US). While fetal bovine serum, 3-(4,5-dimethylthiazol-2-yl)-2,5-diphenyl tetrazolium bromide) called MTT were procured from Thermo Fisher scientific (UK). Pierce™ chromogenic endotoxin quant kit contained lyophilized *E.coli* (0111: B4), lyophilized amebocyte lysate (LAL), lyophilized chromogenic substrate, endotoxin-free water were purchased from Thermo Scientific.

2.2 Preparation of nanocrystalline cellulose

The raw kenaf bast fibers underwent an extraction process to obtain NCC, and established method used in our laboratory [17]. The retting of raw kenaf bast fibers were done by soaking them overnight in distilled water and then filtered several times with subsequent drying at 37 °C in the oven until fully dried. The dried kenaf bast fibers were then ground with a mechanical grinder until they became powder, and the powdered kenaf bast fibers were stored at room temperature in a closed container until further treatment. The powdered kenaf bast fibers were treated with 5% (w/v) NaOH at 80 °C for 2 h in a water bath. The fibers were then thoroughly washed and filtered with distilled water to remove the residue alkali. The procedure was repeated three times. This alkali treatment was performed to eliminate the hemicellulose, lignin and other impurities from the kenaf bast fibers. The fiber solution ratio used in all treatments was 1:20 (g/mL). After the alkali treatment, the alkali-treated pulp then undergone the bleaching process. The bleaching was done by using a combination of glacial acetic acid (3%) and sodium chlorite (2%) as the bleaching agents with 1:1 ratio. This bleaching process was conducted at 80 °C for 3 h and the process was repeated 5 times until the pulp became completely white. The bleached white pulp was washed several times with distilled water. Then, the bleached pulp was dried in the oven until completely dry.

After drying the dried pulp appeared white and clumped, and it was ground to obtain the powder. 5 g of the bleached pulp was hydrolysed in 30% sulphuric acid (H_2SO_4) with 1:20 pulp-to-acid ratio at 50 °C for 1 h with constant stirring. After 1 h, twofold of cold distilled water was added to the suspension to terminate the hydrolysis reaction, and the suspension was left to cool. The suspension appeared milky white in color with the pulp dissolved in acid. Then, the diluted suspension was centrifuged at 12,000 rpm for 30 min. This step was repeated five times to remove the acid. The collected precipitate was placed in the dialysis tube (MWCO 11 KDa; cellulose acetate) and submerged in distilled water under slow stirring until complete neutralization (water pH = 7). The suspension of the fine fibers was ultra-sonicated at 20 kHz frequency with 80% amplitude for 5 min. This ultra-sonicate process was conducted under ice to prevent overheating. The resulting suspension of nanofibers was freeze-dried and stored at − 80 °C for further used.

2.3 Formation of activated carbon-nanocrystalline cellulose hydrogel (AC/NCC hydrogel)

Firstly, 150 mg chitosan powder, 0.4% (w/v) of NCC and 0.1% (w/v) AC were added to 5 mL distilled water. The resulting dispersion was ultra-sonicated at 20 kHz frequency with 40% amplitude for 5 min to homogenize the NCC and AC in the mixture. The solution was then allowed to mix on a shaker for 1 h and 1% acetic acid was added to further solubilize the CS and the mixture. The solution was stirred for another 5 h until complete dissolution was achieved. To prepare a crosslinked hydrogel, 20 µL of 0.5% (w/v) genipin solution was added to the solution and stirred for another 30 min. The mixtures were incubated at 37 °C for 24 h to facilitate the gelation. The formed hydrogel was stored at room temperature and away from direct light until further characterization. The viscous solution was then stored at room temperature to form hydrogel and for further characterization. The summary of the formation of AC/NCC hydrogel is illustrated in Fig. 1.

For study comparison purposes, a blank hydrogel was prepared with the same procedure above but without the addition of NCC. This blank hydrogel was used as a negative control for the assessment of rheological properties, spreading ability, and swelling study, while Intrasite hydrogel (commercial) was used as a positive control. Another control hydrogel without AC was also prepared for the toxin removal study.

2.4 Hydrogel characterization

2.4.1 2.4.1. Fourier transform infrared spectroscopy (FTIR) analysis

The chemical functional groups of raw materials including NCC, AC and CS were assessed using a Fourier Transform Infrared (FTIR) spectrometer (Perkin Elmer spectrometer 100) using a Perkin Elmer Universal ATR (Attenuated Total Reflection) sampling assembly. The sample was placed in full contact with the high reflective index prism at the top of the compartment and maximum force was applied by using an ATR pressure clamp to allow optimum contact with the sample. The materials were analyzed in transmittance mode with 32 scans and the wavenumber within the range of 4000–650 cm^{-1}.

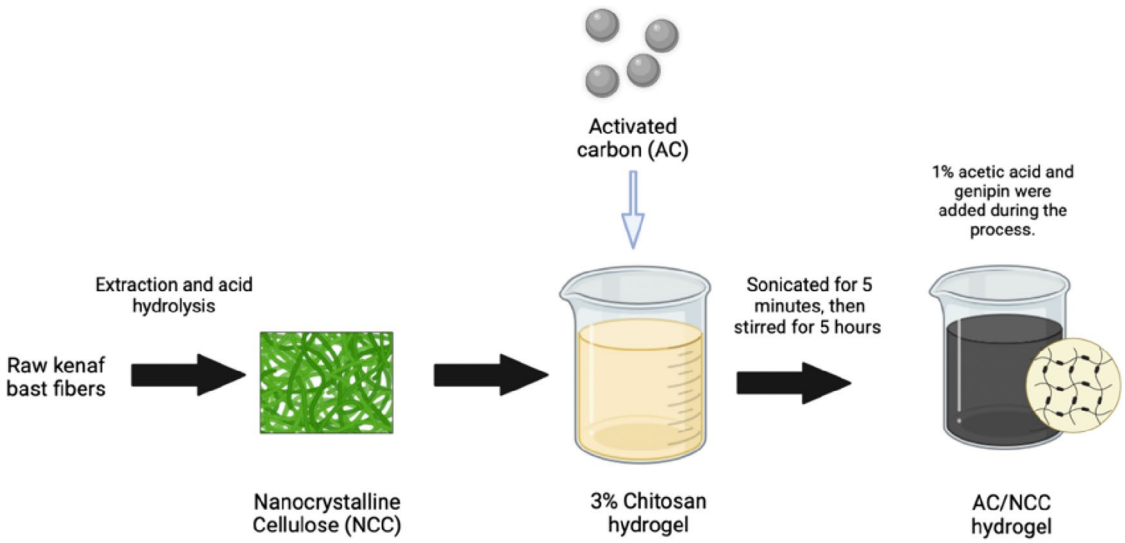

Fig. 1 Schematic diagram of AC/NCC hydrogel formation

2.4.2 2.4.2. Zeta potential

Zeta potential (surface charge) of AC. NCC, CS was characterized using Malvern Zetasizer Nano ZS (Malvern Instrument, UK). Samples were measured in triplicate and the data are presented as mean ± standard deviation (SD).

2.5 Mechanical properties

2.5.1 Hydrogel spreadibility

A glass plate was pre-marked with a 1 cm diameter of circle and 0.1 g of the formulation was placed on the circle with a second glass plate was put over the hydrogel. Then, 500 g of weight was placed on top of the glass plate for 5 min. The diameter of the spreading of the hydrogel was measured and recorded. The spreadability of the formulated hydrogel was compared to that of the commercial hydrogel (Intrasite hydrogel). Each formulation was carried out in triplicate.

2.5.2 Rheological properties

Rheology measurement was made using a rheometer (Bohlin Gemini Rotonetic Drive 2, Malvern, USA). Data analysis was made using Bohlin Software: Gemini 200 software. A plate-plate system was used, and the spindle specification was a parallel plate (PP40 Ti) with a diameter of 4 cm. The distance between the plates was 0.5 mm and the measuring temperature was 25 °C. Approximately 2 g of hydrogel sample was applied to fill the gap between the plates. The flow behavior was measured using the up-and-down rotational controlled ramp test. The shear rate ranging from 0.01 to 100 s^{-1} is applied for 5 to 10 min with a time delay of 10 s between successive measurements. The results for viscosity measurements are reported at maximum shear rate (at 100 s^{-1}).

2.6 Swelling behavior

The swelling degree of the hydrogel was evaluated by the water uptake as a function of time. The test method was modified from Matthews et al. [27]. A 4% w/v gelatine medium was used as the swelling medium to mimic the wound surface. The gelatine medium was made by adding gelatine powder to distilled water at 60 °C with continuous stirring until a clear solution was formed. The clear solution was removed from the heat, and an equal mass (20 g) of the solution was poured into an individual petri dish, covered and allowed to cool to room temperature (25 °C) overnight. Approximately 0.1 g of hydrogel was placed above a gelatine medium, an in vitro wound simulation model. The swelling of the hydrogel was recorded at intervals of 15 min, 30 min, 1, 2, 3 h (until equilibrium was established). The percentage swelling at each time point was calculated using equation:

$$\text{Swelling } \% = \left(D_t - D_0/D_0\right) \times 100 \quad (1)$$

where D_0 is the initial diameter, and D_t is the swelled diameter at time interval t.

2.7 Cytotoxicity study

The cytotoxicity was determined by using MTT assay (3- [4, 5- dimethylthiazol-2-yl]-2, 5-diphenyltetrazolium bromide) on normal human dermal fibroblast (NHDF) and keratinocytes cell (HaCaT) cells. Cell culture with a concentration of 2×10^4 cells/mL was prepared and was plated (100 µL/well) onto 96-well plates. The diluted ranges of AC/NCC hydrogel were added to each well with identified AC concentration: 15.625, 31.25, 62.5, 125, 250, 500 mg/mL further incubated for 24 h. A control group with no treatment was also included. After that, the MTT solution was added to the cells and continued for incubation for a further 3 h. The MTT assays were performed in triplicate. After the solubilization of the purple formazan crystals using DMSO was completed, the optical density of samples was measured using a microplate reader at a wavelength of 570 nm. The percentage of cell viability was determined using the following formula:

$$\% \text{ cell viability} = \frac{\text{Absorbance of sample}}{\text{Absorbance of control}} \times 100 \quad (2)$$

2.8 Toxin removal study

The Pierce™ chromogenic endotoxin quant kit was used and prepared based on the manufacturer's guide with some modifications. Lipopolysaccharide (LPS) solutions were prepared at 10 EU/mL stock of lyophilized *E.coli*. The test was performed using a 96-well plate microtiter plate in triplicate and reaction was measured over 45 min. For each well, 50 µL AC/NCC hydrogel or control hydrogel (without AC) on the lyophilized *E.coli* was applied. Then, the solution was mixed with 50 µL of LAL and incubated for 14 min. Next, the chromogenic substrate was added. After 50 µL of 25% acetic acid was added to each well to stop reaction, the optical density was read and analyzed at 405 nm. Equations (3) were used to measure the efficiency of endotoxin removal in this experiment based on the calibration curve. Five-point calibration line ranging from 1.0 to 0.1 endotoxin unit per mL (EU/mL) of lyophilized *E.coli* with application of LAL and lyophilized chromogenic substrate was also prepared. The calibration line Eq. (3) was calculated by plotting absorbance versus lyophilized *E.coli* concentrations.

$$y = 1.11381x + 0.1596 \quad (3)$$

y is the absorbance of lyophilized *E. coli* and x is the concentration of lyophilized *E. coli* in mg/mL.

The endotoxin removal efficiency was calculated for experiments in 1.0 EU/mL and 0.1 EU/mL endotoxin concentration and experiment by Eq. (4):

$$E = \left(\frac{C_0 - C}{C_0}\right) \times 100 \quad (4)$$

E = toxin removal efficiency in percentage (%)
C_0 = endotoxin concentrations measured in stock solution at 405 nm
C = endotoxin concentrations measured in sample at 405 nm

2.9 Statistical analysis

Statistical analysis was performed using one-way ANOVA, followed by Tukey's multiple-comparisons test, by using GraphPad Prism version 5.00 (GraphPad Software, USA). Statistical significance was accepted at $p < 0.05$.

3 Results and discussion

3.1 Fourier transform infrared (FTIR) spectra analysis

Fourier transform infrared (FTIR) is one of the essential instruments for the analysis of functional groups and to detect the chemical interaction between compounds. FTIR was employed to analyze the structural changes that occurred after the formation of AC and NCC together with CS. Figure 2 represents the FTIR spectra of pure NCC, AC, CS, and AC/NCC hydrogel in the range of 550–4000 cm^{-1}. All spectra detected a broad and intense peak at 3300 cm^{-1} region which is attributed to the characteristic of polysaccharides hydroxyl bonds. The bands found in the CS spectrum corroborated with those reported by others [17, 28, 29]. A strong broad absorption located at 3323 cm^{-1} of NCC is attributed to the O–H stretching vibration in the celluloses. The peaks at 1000–1030 cm^{-1} region are caused by stretching vibrations of the C–O–C pyranose ring peak in both NCC and CS. After incorporation with AC, the O–H vibration shifts to a lower wavenumber (3293 cm^{-1}, AC/NCC), indicating that the increase in -OH stretching due to intermolecular bonding with water in the AC/NCC

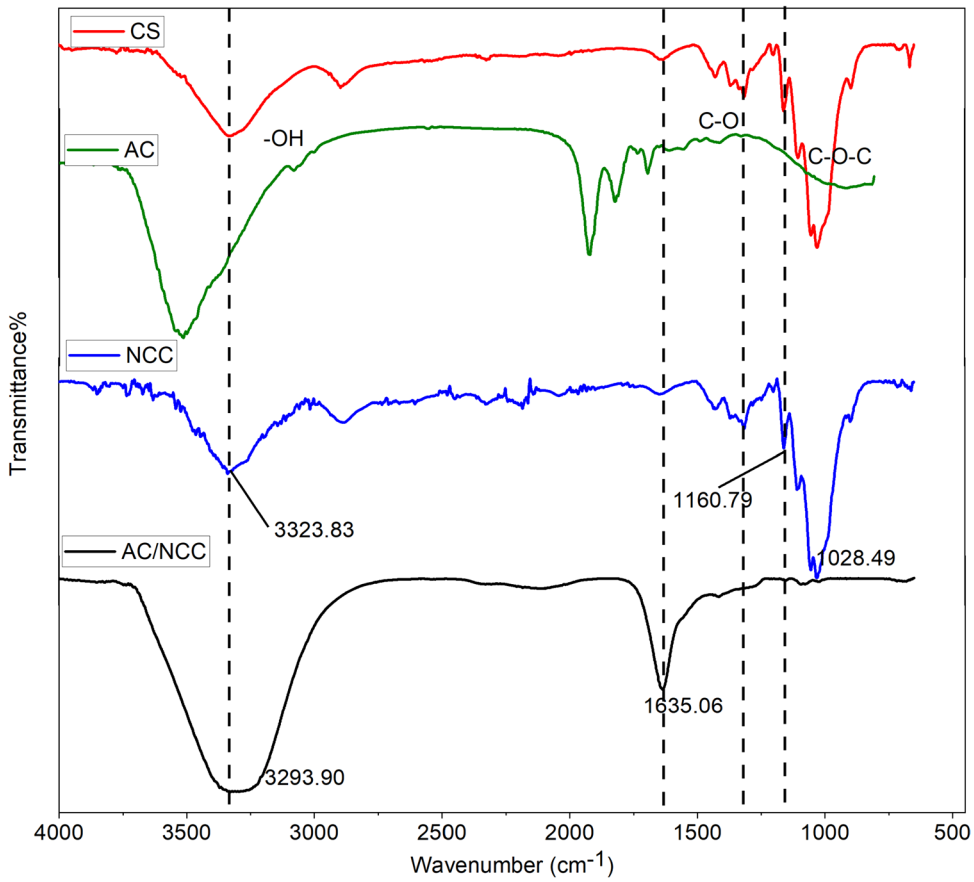

Fig. 2 FTIR spectra of raw CS, AC, NCC and AC/NCC hydrogel

hydrogels [30–32]. The reduction of C–O–C pyranose ring peak in AC/NCC hydrogel spectrum may be attributed to the small amount of AC and NCC presence in the hydrogel (as compared to pure AC and pure NCC powders) which produced less vibrational energy. The 1635 cm^{-1} peak as seen in AC/NCC hydrogel is likely due to the CH_3 bending of the methyl ester and C = C ring stretching of the genipin or -OH bending due to interaction with water molecules. The FTIR peaks suggest that the formation of AC/NCC is a physical interaction.

3.2 Zeta potential

The zeta potential measurements were conducted to determine the surface properties and stability of AC/NCC hydrogel. The zeta potential of AC/NCC hydrogel was measured at $+62.0 \pm 0.03$ mV. The anionic AC and NCC are found suitable to form composite hydrogels with cationic CS. The abundance of hydroxyl groups in NCC and AC are responsible for the negative charges that bonded with CS via the electrostatic interaction of protonation of NH_2 on CS and hydroxyl groups. The zeta potential of AC/NCC showed that AC and NCC were stabilized when formed with CS which acts as a donor charge. The CS could provide substantial electrostatic stability to the composites by rendering surface charge adequately. The composite with a stable surface charged potential would give the best antibacterial effect towards bacteria [33].

3.3 Hydrogel spreadibility and rheological properties

The spreading ability (spreadability), also known as hydrogel retention, of a pharmaceutical hydrogel is an important factor contributing to the therapy compliance of the patient with treatment [34]. The spreading ability of hydrogel can also influence the standard dose of a medicated formulation and the therapeutic efficacy to formulate a hydrogel. Therefore, a hydrogel must possess good spreadability characteristics to satisfy and meet the ideal quality as a topical application [35].

The spreadability of the AC/NCC hydrogel, blank hydrogel (i.e. without NCC) and Intrasite gel is shown in Fig. 3. The AC/NCC formulation, Intrasite and blank hydrogel show a diameter of 2.0 ± 0.1 cm, 1.8 ± 0.1 cm and 3.2 ± 0.1 cm, respectively. The spreadability of AC/NCC hydrogel and Intrasite gel were comparable but significantly lower compared to blank hydrogel. This indicates that the NCC has hindered the flow of the hydrogel and behaves as nanofillers to the hydrogel system. Spreadability test was a test designed to measure the ability of the hydrogel to spread on that area when applied to the skin or affected part. The spreadability of hydrogel indirectly indicates the retention

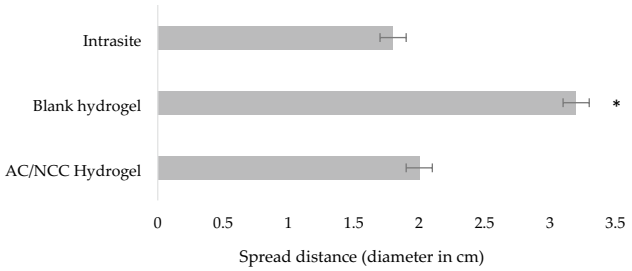

Fig. 3 Hydrogel spreadibility. Data is expressed as Average ± SD, $n = 3$. *denotes the data is significantly different from the AC/NCC hydrogel ($p < 0.05$)

of the hydrogel on the skin. The larger the diameter, the less resistance it is for the hydrogel to flow and vice versa. This study also shows an indication that the AC/NCC hydrogel is able to adhere to the wound site without flowing to other areas on the skin (similar to Intrasite gel). The lower spreadability values of the hydrogel may be attributed to the higher viscosity of such formulations as discussed in the next section below.

Figure 4 depicts the flow curves of the hydrogel formulations. The rheological assessment shows that all hydrogels exhibit pseudoplastic properties. The shear thinning properties of the formulations showed the viscosities decreased with increasing shear rate with no yield value. Pseudoplastic hydrogels are generally thick at rest and the viscosity reduces when the shear stress is applied [36]. When the external stress is removed, the hydrogels then return to their viscous state. The high shearing action on the long chain molecules of linear polymer also showed that disarranged molecules begin to align their long axis in the direction of flow with the release of solvent from the hydrogel matrix as the shearing stress increases [36, 37]. These shear-thinning properties are essential to allow appropriate removal from container.

At a shear rate of 100 s^{-1}, the hydrogels exhibit average apparent viscosities, η_{app}, ranging from 1.15 ± 0.02 Pa.s to 1.22 ± 0.01 Pa.s whereas the Intrasite gel was measured at 1.10 ± 0.01 Pa.s (Fig. 4). The average apparent viscosities of AC/NCC and blank hydrogel (without NCC) formulations were statistically significantly different from Intrasite ($P < 0.0001$). There was an increase in the apparent viscosity when the concentration of NCC was added to the gel formulations. The increased in the viscosity of the formulations was probably due to NCC behaves as nanofillers which retards the CS polymer movements within the hydrogel matrix. The rheological data corroborated with the spreadibility results. The mechanical studies have inferred that besides having good spreadability for the ease of application, the AC/NCC hydrogels have the ability to retained at the application site without draining away which is important

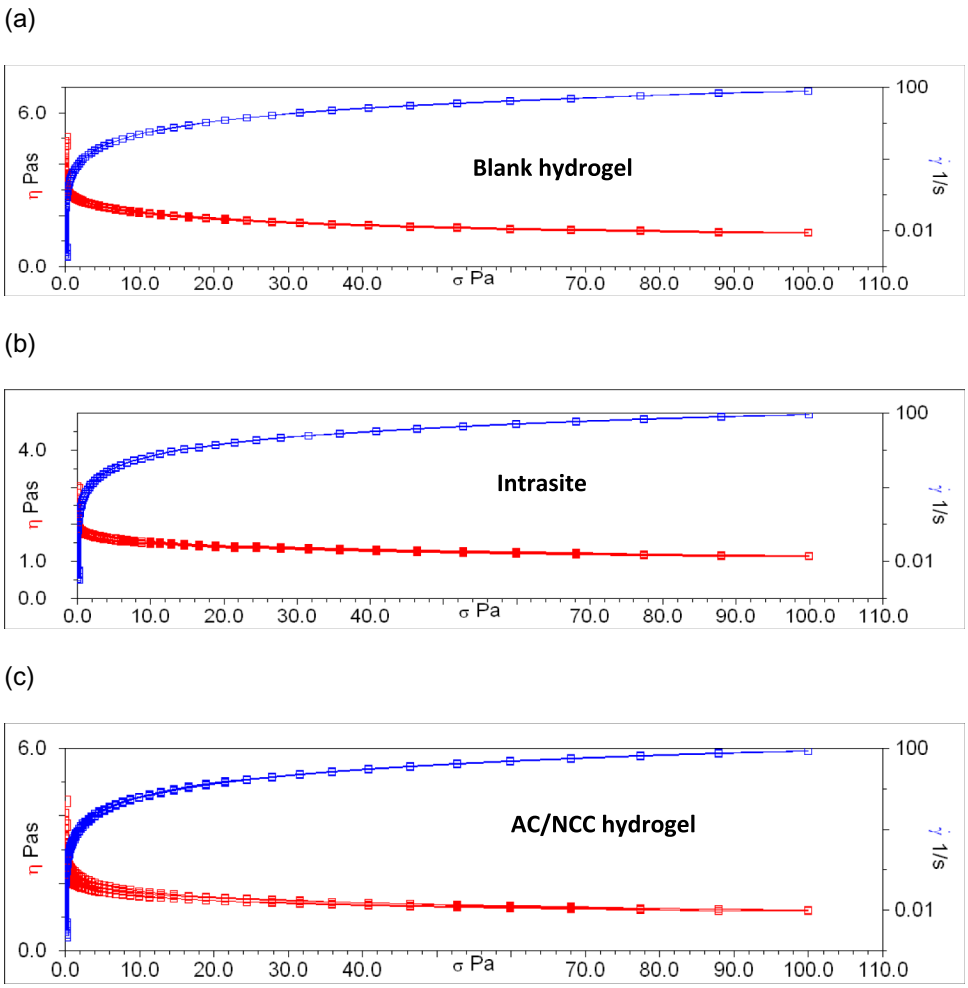

Fig. 4 Flow curves of (**a**) Blank CS hydrogel ($\eta_{app} = 1.10 \pm 0.01$ Pa.s) (**b**) Intrasite ($\eta_{app} = 1.15 \pm 0.02$ Pa.s) and (**c**) AC/NCC hydrogel ($\eta_{app} = 1.22 \pm 0.01$ Pa.s). η_{app} or apparent viscosity is taken at the apex of the flow curve where shear rate at 100 s^{-1}

for wound application, particularly vital for deep wounds with large amount of exudates.

3.4 Swelling behavior

The swelling behavior of hydrogel dressing is an important feature since an appropriate swelling degree will maintain the required moist environment of wound and protect it from extreme dehydration [38]. The swelling degree of the hydrogels are shown in Fig. 5. The result shows a gradual increase of swelling degree in all hydrogels for the 1st hour and plateau thereafter till 3 h. As expected, the incorporation of NCC significantly reduced ($p < 0.05$) the swelling property of the CS hydrogel as compared to AC/NCC hydrogels. At 1 h, the swelling % of the blank hydrogel was found to be 219%, and incorporation of NCC resulted in a decrease of the swelling % of the hydrogels approximately by 50%. The swelling behavior of the hydrogels was also inversely corelated with rheological properties (Fig. 4), i.e. the higher the hydrogel viscosity, the slower the hydrogel swells.

Same decreasing achieved by Huq and colleagues [39] by incorporation of (1%–8% wt) of NCC extracted from

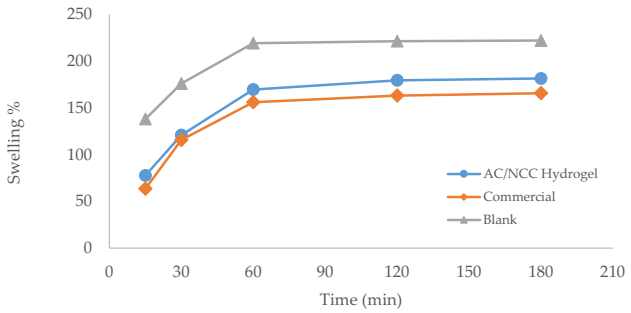

Fig. 5 Swelling behavior comparison between AC/HCC Hydrogel and commercial Intrasite hydrogel

softwood kraft pulp into alginate-based film. In this study, the swelling percentage was significantly reduced from 187% for pure alginate hydrogel film to 99% and 111%, whin reinforced by 5%,8% NC, respectively. Similarly. Deepa et al. (2016) reported that the swelling percentage significantly reduced when incorporating cellulose nanofibrils into alginate film. The result showed that the swelling percentage of the control film was 124% compared to 65%

and 77% after the incorporation of 10% and 15% NCC, respectively [40].

Hydrogel swelling behavior is related to the polymer hydrophilic composition and cross-linking degree of the matrix [41]. The hydrogels with higher crosslinking density showed a lower swelling ratio. This is due to the difficulty of water molecules to pass through polymers with high cross-link density which causes smaller pore size, less space and a low swelling ratio. In addition, NCC with its hydrophobic molecular skeleton can decrease the entirety of the hydrophilicity of the matrix network [42]. The decrease in swelling degree can be due to the formation of strong interactions between the matrix and the NCC nanofiller [17].

3.5 Cytotoxicity study

The MTT assay is a tool to measure cellular metabolic activity as an indicator of cell viability, proliferation and cytotoxicity. This assay is largely used for screening toxic and harmless compounds, quick analysis with high reproducibility. The fibroblast cell (NHDF) and keratinocytes cell (HaCaT) are different skin cells and were used to evaluate the cytotoxicity of wound dressing material. From Fig. 6, the experiment showed 100–160% cell viability of HaCaT and NHDF when treated up to 250 mg/mL of AC in the hydrogel. Based on the ISO guidelines for medical devices and biomaterials, for materials such as wound dressing to be accepted as biocompatible, the cell viability after exposure should be $\geq 70\%$ [43]. Hence the result suggests that AC/NCC hydrogel formulated with AC up to 250 mg/mL concentration exhibits good cell biocompatibility. The AC/NCC hydrogel is regarded as non-toxic and safe to be applied to wounds. AC is regarded as GRAS (Generally Recognized as Safe) by the FDA. Thus, a combination of AC/NCC shows that hydrogel can promote wound healing without being toxic to host tissues.

3.6 Endotoxin removal study

Endotoxin is a complex lipopolysaccharide found in Gram-negative bacteria's outer cell membrane. Endotoxins are routinely released by bacteria as they grow and divide in their normal life cycle, but large volumes of endotoxins can be released during cell lysis and have been associated with diseases such as delayed wound healing. This chromogenic quantitative LAL assay was conducted to investigate the toxin removal efficiency of the AC/NCC hydrogel at two conditions: low and high endotoxins levels, measured at 0.1 and 1.0 endotoxins units per milliliter (EU/mL), respectively. This assay uses the amebocyte lysate method to measure the interaction of endotoxins with proenzyme Factor C. Endotoxin levels are determined by measuring the activity of Factor C in the presence of the colorless chromogenic synthetic peptide substrate (Ac-Ile-Glu-Ala-Arg-pNA) that releases p-nitroaniline (pNA) after proteolysis, producing a yellow color that can be measured at an absorbance of 405 nm.

The toxin removal efficiency (in %) of AC/NCC hydrogels is presented in Fig. 7. The result showed that the hydrogel effectively removed $84.8 \pm 4.3\%$ toxins when placed in wells with low endotoxin levels. However, at wells with high endotoxins level, the AC/NCC hydrogel was only able to eliminate 49.4% of LPS. And there was no significant difference in antitoxin activity between the AC/NCC hydrogel and the control. As this assay is a chromogenic quantitative assay, the amount of endotoxin adsorbed by the AC was probably too low to be measured by spectrophotometry due

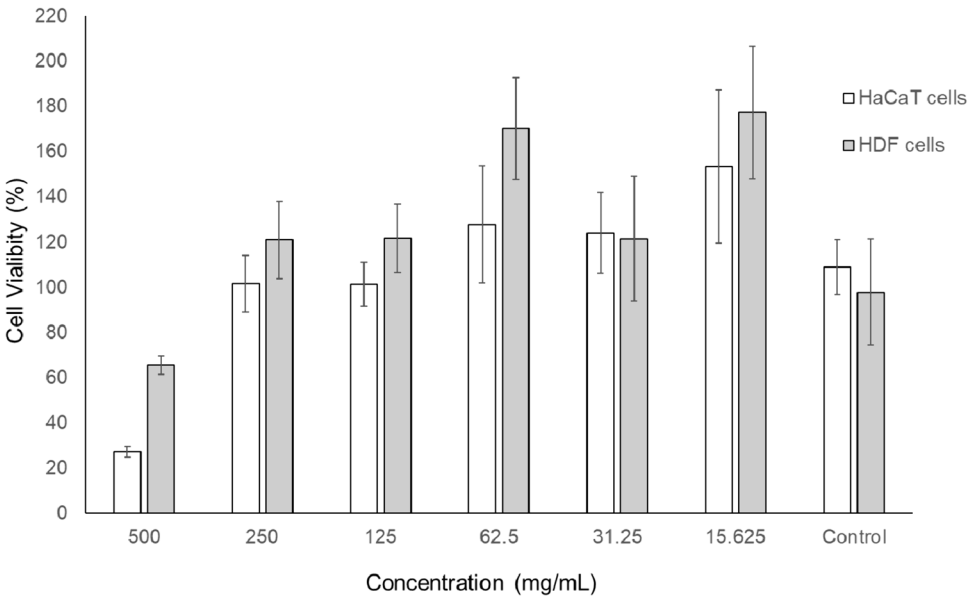

Fig. 6 Cytotoxicity of AC/NCC towards HaCaT and NHDF cells

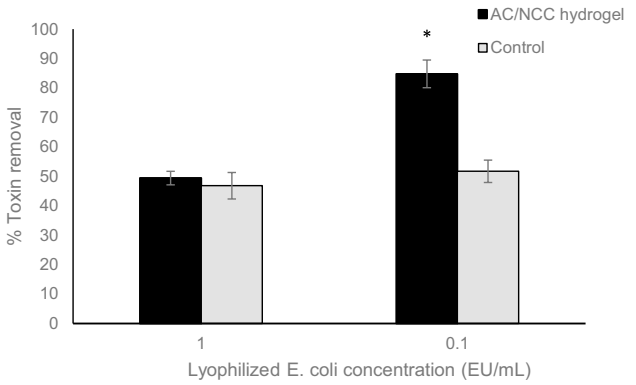

Fig. 7 The percentage of toxin removal from AC/NCC-0.25% in different concentrations of lyophilized *E. coli*. *denotes the data is significantly different from control hydrogel ($p < 0.05$)

to the high level of endotoxins in the solution (solution is dark yellow in colour). The fact that the control hydrogels (without AC) also show antitoxin effects (approx. 50% toxins removed) is likely due to the presence of CS. CS may have an antitoxins effect as it is a cationic polymer that can interact electrostatically negatively charged LPS [44].

Interestingly, the AC/NCC hydrogel was shown to be effective in eliminating endotoxins. This is likely attributed to the high density of pores created by a high surface area of AC as well as the cationic chitosan polymers. The high surface area of AC, which can specifically bind and reduce endotoxin levels, may be a useful adjunct to topical wound management and infection control [45]. Another probable reason that AC possessed good endotoxin removal efficiency is because AC is a non-specific adsorbent with pores [15]. The placement of an AC/NCC at the surface of a wound could result in the physical adsorption of bacteria as well as their freely secreted exotoxin and endotoxin from the wound surface and from the wound fluid [46]. This will in turn accelerate the healing rate especially of chronic wounds. The levels of endotoxins (0.1 and 1.0 EU/mL) tested in this study by no means were associated with the actual level of endotoxins in infected wounds. It was carried out at these concentrations for the sake of comparison at high and low endotoxins levels. However, these experimental conditions can be extrapolated to represent the different degrees of infections in the wounds.

A dressing that combines the properties of hydrogels and AC could be very beneficial for the treatment of malodorous wounds. The AC in the hydrogel can simultaneously adsorb the endotoxins, malodours and any degradation products at the wound site. Osmokrovica and co-workers [47] developed hydrogel beads using Zinc-alginate hydrogel loaded with AC particles and was intended for wound treatments in which the hydrogel will absorb the wound exudate while the efficient and simultaneous release of the active agents (Zinc and AC). AC's function was to adsorb wound toxins, malodour molecules and zinc ions will exert antimicrobial effects and enhancement of wound healing [47]. While the experimental outcomes for the AC-containing wound dressings are commendable, most AC-loaded formulations in the literature lack endotoxins removal assay.

From previous studies, it was found that the larger MW (> 30 kDa) CS generally have anti-inflammatory activity whereas smaller MW (< 30 kDa) or oligomer range CS have pro-inflammatory activity [48–50]. The CS used in this study has M_W 50–190 kDa. So here we can infer that the AC/NCC hydrogel may also possess some pro-inflammatory activity. We recommend that AC/NCC hydrogel dressing be used on wounds that are still at the initial or inflammatory phase of the wound healing stage. This will be beneficial because the CS in hydrogel will stimulate pro-inflammatory cytokines such as IL-1β, IL-6, and TNF-α that play vital roles in recruiting cells for debris clearance and the elevation of growth factors at the initial stages of wound healing. However, it is noteworthy that most past research which studied the relationship between inflammation activity and chitosan MW were based on in vitro or cell assays [50]. Dayvdova and co-workers showed that CS with MW 20 kD exhibits higher affinity to LPS than CS with MW 140 kD [44]. Future formulation optimization of AC/NCC hydrogel can be carried out with low MW CS. However, this may render the hydrogel to be more suitable for the later stage of wound healing where anti-inflammatory activities are crucial for wound healing.

4 Conclusion

In conclusion, AC/NCC hydrogel was developed to address the delayed wound healing problem associated with bacterial infection as well as endotoxin released on the wound site. In this study, AC/NCC was shown to possess desirable spreadibility and rheological properties when compared to the commercial hydrogel dressing (Intrasite gel). FTIR study confirmed the formation of AC/NCC with CS was present and that AC, NCC and CS interactions are physical in nature. The zeta potential of AC/NCC showed that AC and NCC was stabilized when formed with CS act as donor charge. In vitro study revealed that AC/NCC hydrogel found to be non-toxic to host tissue (> 100% NHDF and HaCaT cell viability) with concentration below 250 mg/mL. The result of the endotoxin removal assay indicated that AC/NCC hydrogel was able to remove the endotoxin of more than 85% when treated with 0.1EU/ml LPS. Thus, it can be deduced that AC/NCC hydrogel can be a promising candidate to eliminate endotoxin from infected wounds and accelerate wound healing. The encouraging in vitro

data warrants the AC/NCC hydrogel dressing for in vivo efficacy testing as further investigations.

Acknowledgements The authors are grateful to the National Kenaf and Tobacco Board (LKTN) and Noble Health Sdn Bhd. Hydrogel formation work and facilities were provided by the Faculty of Pharmacy, UKM. This research was funded by a UKM research grant (grant no. GUP-2019-003).

Declarations

Conflict of interest On behalf of all authors, the corresponding author states that there is no conflict of interest.

References

1. M. Olsson, K. Järbrink, U. Divakar, R. Bajpai, Z. Upton, A. Schmidtchen, J. Car, The humanistic and economic burden of chronic wounds: a systematic review. Wound Repair Regen. **27**, 114–125 (2019). https://doi.org/10.1111/wrr.12683
2. M.G. Rippon, S. Westgate, A.A. Rogers, Implications of endotoxins in wound healing: a narrative review. J. Wound Care **31**, 380–392 (2022). https://doi.org/10.12968/jowc.2022.31.5.380
3. R. Yuan, S. Geng, K. Chen, N. Diao, H.W. Chu, L. Li, Low-grade inflammatory polarization of monocytes impairs wound healing. J. Pathol. **238**, 571–583 (2016). https://doi.org/10.1002/path.4680
4. N.N. Zulkefli, L.S. Mathuray Veeran, A.M.I. Noor Azam, M.S. Masdar, W.N.R. Wan Isahak, Effect of bimetallic-activated carbon impregnation on adsorption-desorption performance for hydrogen sulfide (H2S) capture. Materials **15**, 5409 (2022). https://doi.org/10.3390/ma15155409
5. W.N. Adira Wan Khalit, T.S. Marliza, N. Asikin-Mijan, M.S. Gamal, M.I. Saiman, M.L. Ibrahim, Y.H. Taufiq-Yap, Development of bimetallic nickel-based catalysts supported on activated carbon for green fuel production. RSC Adv. **10**, 37218–37232 (2020). https://doi.org/10.1039/D0RA06302A
6. S.K. Lakkaboyana, S. Khantong, N.K. Asmel, A. Yuzir, W.Z. Wan Yaacob, Synthesis of copper oxide nanowires-activated carbon (AC@ CuO-NWs) and applied for removal methylene blue from aqueous solution: kinetics, isotherms, and thermodynamics. J. Inorg. Organomet. Polym. Mater. **29**, 1658–1668 (2019)
7. A.M. Lazim, M. Hilman, S. Saroni, N. Muslihuddin, A. Kamil, A.A. Rahman, A.H. Yusoff, M. Mohamed, N. Haida, M. Kaus, E. Kalkornsurapranee, Impregnation of liquid natural rubber (LNR) foam with activated carbon for enhancing oil removal from water. Desalin. Water Treat. **187**, 232–240 (2020). https://doi.org/10.5004/dwt.2020.25393
8. B.K. Pramanik, S.K. Pramanik, F. Suja, A comparative study of coagulation, granular- and powdered-activated carbon for the removal of perfluorooctane sulfonate and perfluorooctanoate in drinking water treatment. Environ. Technol. **36**, 2610–2617 (2015). https://doi.org/10.1080/09593330.2015.1040079
9. A.F. Ismail, M.S. Yim, Investigation of activated carbon adsorbent electrode for electrosorption-based uranium extraction from seawater. Nucl. Eng. Technol. **47**, 579–587 (2015). https://doi.org/10.1016/J.NET.2015.02.002
10. M. Minsart, A. Mignon, A. Arslan, I.U. Allan, S. van Vlierberghe, P. Dubruel, Activated carbon containing PEG-based hydrogels as novel candidate dressings for the treatment of malodorous wounds. Macromol. Mater. Eng. **306**, 2000529 (2021). https://doi.org/10.1002/mame.202000529
11. J.C. Kerihuel, Effect of activated charcoal dressings on healing outcomes of chronic wounds. J. Wound Care **19**, 208–214 (2010). https://doi.org/10.12968/jowc.2010.19.5.48047
12. M.C. Murphy, S. Patel, G.J. Phillips, J.G. Davies, A.W. Lloyd, V.M. Gun'ko, S.V. Mikhalovsky, Adsorption of inflammatory cytokines and endotoxin by mesoporous polymers and activated carbons, in *Characterization of Porous Solids*, vol 6, ed. by F. Rodriguez-Reinoso, B. McEnaney, J. Rouquerol, K. Unger (Elsevier, Amsterdam, 2002), pp. 515–520. https://doi.org/10.1016/S0167-2991(02)80175-6
13. S.K. Maitra, T.T. Yoshikawa, L.B. Guze, M.C. Schotz, Properties of binding of Escherichia coli endotoxin to various matrices. J. Clin. Microbiol. **13**, 49–53 (1981). https://doi.org/10.1128/jcm.13.1.49-53.1981
14. B. Ditter, R. Urbaschek, B. Urbaschek, Ability of various adsorbents to bind endotoxins in vitro and to prevent orally induced endotoxemia in mice. Gastroenterology **84**, 1547–1552 (1983). https://doi.org/10.1016/0016-5085(83)90378-5
15. K. Naka, S. Watarai, Tana, K. Inoue, Y. Kodama, K. Oguma, T. Yasuda, H. Kodama, Adsorption effect of activated charcoal on enterohemorrhagic Escherichia coli. J. Vet. Med. Sci. **63**, 281–285 (2001). https://doi.org/10.1292/jvms.63.281
16. N. Ma, D.Y. Cheung, J.T. Butcher, Incorporating nanocrystalline cellulose into a multifunctional hydrogel for heart valve tissue engineering applications. J. Biomed. Mater. Res. A **110**, 76–91 (2022). https://doi.org/10.1002/jbm.a.37267
17. P. Bhatnagar, J.X. Law, S.F. Ng, Chitosan reinforced with Kenaf nanocrystalline cellulose as an effective carrier for the delivery of platelet lysate in the acceleration of wound healing. Polymers (Basel) **13**, 4392 (2021). https://doi.org/10.3390/polym13244392
18. R. Singla, S. Soni, V. Patial, P.M. Kulurkar, A. Kumari, S. Mahesh, Y.S. Padwad, S.K. Yadav, In vivo diabetic wound healing potential of nanobiocomposites containing bamboo cellulose nanocrystals impregnated with silver nanoparticles. Int. J. Biol. Macromol. **105**, 45–55 (2017). https://doi.org/10.1016/j.ijbiomac.2017.06.109
19. D. Thomas, M.S. Nath, N. Mathew, R. Reshmy, E. Philip, M.S. Latha, Alginate film modified with aloevera gel and cellulose nanocrystals for wound dressing application: preparation, characterization and in vitro evaluation. J Drug Deliv Sci Technol **59**, 101894 (2020). https://doi.org/10.1016/j.jddst.2020.101894
20. N. Akhavan-Kharazian, H. Izadi-Vasafi, Preparation and characterization of chitosan/gelatin/nanocrystalline cellulose/calcium peroxide films for potential wound dressing applications. Int. J. Biol. Macromol. **133**, 881–891 (2019). https://doi.org/10.1016/j.ijbiomac.2019.04.159
21. O.A. Adeleye, O.A. Bamiro, D.A. Albalawi, A.S. Alotaibi, H. Iqbal, S. Sanyaolu, M.N. Femi-Oyewo, K.O. Sodeinde, Z.S. Yahaya, G. Thiripuranathar, F. Menaa, Characterizations of alpha-cellulose and microcrystalline cellulose isolated from cocoa pod husk as a potential pharmaceutical excipient. Materials (Nasel) **15**, 5992 (2022). https://doi.org/10.3390/MA15175992
22. N. Zainuddin, I. Ahmad, M.H. Zulfakar, H. Kargarzadeh, S. Ramli, Cetyltrimethylammonium bromide-nanocrystalline cellulose (CTAB-NCC) based microemulsions for enhancement of topical delivery of curcumin. Carbohydr. Polym. **254**, 117401 (2021). https://doi.org/10.1016/J.CARBPOL.2020.117401
23. A.M. Heimbuck, T.R. Priddy-Arrington, M.L. Padgett, C.B. Llamas, H.H. Barnett, B.A. Bunnell, M.E. Caldorera-Moore, Development of responsive chitosan-genipin hydrogels for the treatment of wounds. ACS Appl. Bio Mater. **2**, 2879–2888 (2019). https://doi.org/10.1021/acsabm.9b00266
24. M.A. Matica, F.L. Aachmann, A. Tøndervik, H. Sletta, V. Ostafe, Chitosan as a wound dressing starting material: antimicrobial properties and mode of action. Int. J. Mol. Sci. **20**, 5889 (2019). https://doi.org/10.3390/ijms20235889

25. E. Dalir Aabdolahinia, M. Alipour, M. Aghazadeh, M. Hassanpour, M. Ghorbani, Z. Aghazadeh, An injectable chitosan-based hydrogel reinforced by oxidized nanocrystalline cellulose and mineral trioxide aggregate designed for tooth engineering applications. Cellulose **29**, 3453–3465 (2022). https://doi.org/10.1007/s10570-022-04491-z
26. S.D. Dutta, J. Hexiu, D.K. Patel, K. Ganguly, K.T. Lim, 3D-printed bioactive and biodegradable hydrogel scaffolds of alginate/gelatin/cellulose nanocrystals for tissue engineering. Int. J. Biol. Macromol. **167**, 644–658 (2021). https://doi.org/10.1016/j.ijbiomac.2020.12.011
27. K.H. Matthews, H.N.E. Stevens, A.D. Auffret, M.J. Humphrey, G.M. Eccleston, Lyophilised wafers as a drug delivery system for wound healing containing methylcellulose as a viscosity modifier. Int. J. Pharm. **289**, 51–62 (2005). https://doi.org/10.1016/j.ijpharm.2004.10.022
28. S.G. Anicuta, L. Dobre, M. Stroescu, I.M. Jipa, Fourier transform infrared (FTIR) spectroscopy for characterization of antimicrobial films containing chitosan (2010). https://api.semanticscholar.org/CorpusID:21536945
29. A. Drabczyk, S. Kudłacik-Kramarczyk, M. Głąb, M. Kędzierska, A. Jaromin, D. Mierzwiński, B. Tyliszczak, Physicochemical investigations of chitosan-based hydrogels containing aloe vera designed for biomedical use. Materials **13**, 3073 (2020). https://doi.org/10.3390/ma13143073
30. W. Lan, C.F. Liu, F.X. Yue, R.C. Sun, J.F. Kennedy, Ultrasound-assisted dissolution of cellulose in ionic liquid. Carbohydr. Polym. **86**, 672–677 (2011). https://doi.org/10.1016/j.carbpol.2011.05.013
31. H. Zhang, Y. Xu, Y. Li, Z. Lu, S. Cao, M. Fan, L. Huang, L. Chen, Facile cellulose dissolution and characterization in the newly synthesized 1,3-diallyl-2-ethylimidazolium acetate ionic liquid. Polymers (Basel) **9**, 1–12 (2017). https://doi.org/10.3390/polym9100526
32. A. Drabczyk, S. Kudłacik-Kramarczyk, M. Głab, M. Kedzierska, A. Jaromin, D. Mierzwiński, B. Tyliszczak, Physicochemical investigations of chitosan-based hydrogels containing Aloe vera designed for biomedical use. Materials **13**, 3073 (2020). https://doi.org/10.3390/MA13143073
33. N. Amira, A. Yusof, N.M. Zain, N. Pauzi, Synthesis of chitosan/zinc oxide nanoparticles stabilized by chitosan via microwave heating. Bull. Chem. React. Eng. Catal. **14**, 450–458 (2019). https://doi.org/10.9767/bcrec.14.2.3319.450-458
34. I. Tomictomic, S.M. Miočic, I.P. Pepic, D.Š Šimic, J. Filipovic, F.-G. Grčic, M. González-Álvarez, H. Benson, Efficacy and safety of azelaic acid nanocrystal-loaded in situ hydrogel in the treatment of acne vulgaris. Pharmaceutics **13**, 567 (2021). https://doi.org/10.3390/PHARMACEUTICS13040567
35. H.M. Tawfeek, D.A.E. Abou-Taleb, D.M. Badary, M. Ibrahim, A.A.H. Abdellatif, Pharmaceutical, clinical, and immunohistochemical studies of metformin hydrochloride topical hydrogel for wound healing application. Arch. Dermatol. Res. **312**, 113–121 (2019). https://doi.org/10.1007/S00403-019-01982-1
36. G. Stojkov, Z. Niyazov, F. Picchioni, R.K. Bose, Relationship between structure and rheology of hydrogels for various applications. Gels **7**, 255 (2021). https://doi.org/10.3390/GELS7040255
37. Q. Huang, When polymer chains are highly aligned: a perspective on extensional rheology. Macromolecules **55**, 715–727 (2022). https://doi.org/10.1021/acs.macromol.1c02262
38. N. Roy, N. Saha, T. Kitano, P. Saha, Development and characterization of novel medicated hydrogels for wound dressing. Soft Mater. **8**, 130–148 (2010). https://doi.org/10.1080/15394451003756282
39. T. Huq, S. Salmieri, A. Khan, R.A. Khan, C. Le Tien, B. Riedl, C. Fraschini, J. Bouchard, J. Uribe-Calderon, M.R. Kamal, M. Lacroix, Nanocrystalline cellulose (NCC) reinforced alginate based biodegradable nanocomposite film. Carbohydr. Polym. **90**, 1757–1763 (2012). https://doi.org/10.1016/j.carbpol.2012.07.065
40. B. Deepa, E. Abraham, L.A. Pothan, N. Cordeiro, M. Faria, S. Thomas, Biodegradable nanocomposite films based on sodium alginate and cellulose nanofibrils. Materials **9**, 50 (2016). https://doi.org/10.3390/MA9010050
41. R. da Silva, M. Ganzarolli de Oliveira, Effect of the cross-linking degree on the morphology of poly(NIPAAm-co-AAc) hydrogels. Polymer (Guildf) **48**, 4114–4122 (2007). https://doi.org/10.1016/J.POLYMER.2007.05.010
42. T.V. Patil, D.K. Patel, S.D. Dutta, K. Ganguly, T.S. Santra, K.T. Lim, Nanocellulose, a versatile platform: from the delivery of active molecules to tissue engineering applications. Bioact. Mater. **9**, 566–589 (2022). https://doi.org/10.1016/J.BIOACTMAT.2021.07.006
43. S. Moritz, C. Wiegand, F. Wesarg, N. Hessler, F.A. Müller, D. Kralisch, U.C. Hipler, D. Fischer, Active wound dressings based on bacterial nanocellulose as drug delivery system for octenidine. Int. J. Pharm. **471**, 45–55 (2014). https://doi.org/10.1016/j.ijpharm.2014.04.062
44. V.N. Davydova, I.M. Yermak, V.I. Gorbach, I.N. Krasikova, T.F. Solov'eva, Interaction of bacterial endotoxins with chitosan. Effect of endotoxin structure, chitosan molecular mass, and ionic strength of the solution on the formation of the complex. Biochemistry (Mosc.) **65**, 1082–1090 (2000)
45. M. Awwad, F. Al-Rimawi, K.J.K. Dajani, M. Khamis, S. Nir, R. Karaman, Removal of amoxicillin and cefuroxime axetil by advanced membranes technology, activated carbon and micelle-clay complex. Environ. Technol. **36**, 2069–2078 (2015). https://doi.org/10.1080/09593330.2015.1019935
46. M.J. Illsley, A. Akhmetova, C. Bowyer, T. Nurgozhin, S.V. Mikhalovsky, J. Farrer, P. Dubruel, I.U. Allan, Activated carbon-plasticised agarose composite films for the adsorption of thiol as a model of wound malodour. J. Mater. Sci. Mater. Med. **28**, 1–6 (2017). https://doi.org/10.1007/s10856-017-5964-x
47. A. Osmokrovic, I. Jancic, I. Jankovic-Castvan, P. Petrovic, M. Milenkovic, B. Obradovic, Novel composite zinc-alginate hydrogels with activated charcoal aimed for potential applications in multifunctional primary wound dressings. HEMIJSKA INDUSTRIJA (Chemical Industry) **73**, 37–46 (2019). https://doi.org/10.2298/HEMIND180629003O
48. S.H. Chang, Y.Y. Lin, G.J. Wu, C.H. Huang, G.J. Tsai, Effect of chitosan molecular weight on anti-inflammatory activity in the RAW 264.7 macrophage model. Int. J. Biol. Macromol. **131**, 167–175 (2019). https://doi.org/10.1016/j.ijbiomac.2019.02.066
49. S. Lee, S. Byun, C. Lee, S.H. Park, D. Rudra, Y. Iwakura, Y.J. Lee, S.H. Im, D.S. Hwang, Resolving the mutually exclusive immune responses of chitosan with nanomechanics and immunological assays. Adv. Healthc. Mater. **11**, 2102667 (2022). https://doi.org/10.1002/adhm.202102667
50. S. Lee, L.T. Hao, J. Park, D.X. Oh, D.S. Hwang, Nanochitin and nanochitosan: chitin nanostructure engineering with multiscale properties for biomedical and environmental applications. Adv. Mater. **35**, 2203325 (2023). https://doi.org/10.1002/adma.202203325